Published in final edited form as:
Neuropharmacology. 2011 May ; 60(6): 944–952. doi:10.1016/j.neuropharm.2011.01.039.

Cannabinoid Receptor Activation Modifies NMDA Receptor Mediated Release of Intracellular Calcium: Implications for Endocannabinoid Control of Hippocampal Neural Plasticity

Robert E. Hampson, **Frances Miller**, **Guillermo Palchik**[1], and **Sam A. Deadwyler**
Dept. of Physiology & Pharmacology, Wake Forest University School of Medicine, Winston-Salem, North Carolina, USA

Abstract

Chronic activation or inhibition of cannabinoid receptors (CB1) leads to continuous suppression of neuronal plasticity in hippocampus and other brain regions, suggesting that endocannabinoids may have a functional role in synaptic processes that produce state-dependent transient modulation of hippocampal cell activity. In support of this, it has previously been shown *in vitro* that cannabinoid CB1 receptors modulate second messenger systems in hippocampal neurons that can modulate intracellular ion channels, including channels which release calcium from intracellular stores. Here we demonstrate in hippocampal slices a similar endocannabinoid action on excitatory glutamatergic synapses via modulation of NMDA-receptor mediated intracellular calcium levels in confocal imaged neurons. Calcium entry through glutamatergic NMDA-mediated ion channels increases intracellular calcium concentrations via modulation of release from ryanodine-sensitive channels in endoplasmic reticulum. The studies reported here show that NMDA-elicited increases in Calcium Green fluorescence are enhanced by CB1 receptor antagonists (i.e. rimonabant), and inhibited by CB1 agonists (i.e. WIN 55,212-2). Suppression of endocannabinoid breakdown by either reuptake inhibition (AM404) or fatty-acid amide hydrolase inhibition (URB597) produced suppression of NMDA elicited calcium increases comparable to WIN 55,212-2, while enhancement of calcium release provoked by endocannabinoid receptor antagonists (Rimonabant) was shown to depend on the blockade of CB1 receptor mediated de-phosphorylation of Ryanodine receptors. Such CB1 receptor modulation of NMDA elicited increases in intracellular calcium may account for the respective disruption and enhancement by CB1 agents of trial-specific hippocampal neuron ensemble firing patterns during performance of a short-term memory task, reported previously from this laboratory.

Keywords

Calcium; cannabinoid; n-methyl-d-aspartate; glutamate; second messenger; protein kinase; plasticity; confocal imaging; fluorescence

Corresponding Author: Sam A. Deadwyler, PhD., Wake Forest University Health Sciences, Medical Center Blvd., Winston-Salem NC 27157, Phone: +1-336-716-8540, FAX: +1-336-716-8628, sdeadwylwfubmc.edu.
[1]**Current Address:** Georgetown University School of Medicine, Washington, District of Columbia, USA

1. Introduction

The possible cellular bases for the chronic effects of cannabinoid treatment in recent investigations are related to cannabinoid receptor modulation of synaptic activity in specific neuronal systems (Fowler et al., 2010; Glickfeld and Scanziani, 2006; Hashimotodani et al., 2008; Kim and Alger, 2010; Martin-Garcia et al., 2010). Prior studies have revealed in some systems, interactions between cannabinoid CB1 receptor activation and reductions in synaptic transmission (Chevaleyre and Castillo, 2003; Falenski et al., 2007; Fortin et al., 2004; Pertwee, 2005). A direct action of endocannabinoids on synaptic transmission provides possible explanations for noted incidences of behavioral change due to modulated release of known neurotransmitters or modification of related cellular processes (Foldy et al., 2006; Kim and Alger, 2004; Losonczy et al., 2004; Wilson et al., 2001). Here we provide direct evidence for cannabinoid modulation of hippocampal glutamatergic activation by showing that NMDA-receptor mediated release of intracellular calcium (Ca^{++}), imaged in hippocampal slices, is reduced via CB1 receptor activation by endocannabinoids. The following report shows that the ability of NMDA receptor gated Ca^{++} ions to potentiate calcium-sensitive endoplasmic reticulum Ryanodine (RYR) receptors to release intracellular calcium (Li et al., 2006), is reduced by activation of CB1 receptors. The results support the notion that CB1 receptor activation attenuates synaptic processing in hippocampal neurons by decreasing the potential to modulate the release of intracellular calcium in circumstances where such flexibility is critical for adapting to requirements for successful memory encoding and retrieval (Deadwyler et al., 2007; Deadwyler and Hampson, 2008).

Recent studies have demonstrated the selective disruption of different types of memory following treatment with cannabinoid receptor agonists such as WIN 55 212 (Abush and Akirav, 2009; Kim and Alger, 2010; Manwell et al., 2009). Prior investigations from this laboratory have demonstrated the negative influence of endogenous cannabinoids on the modulation of hippocampal memory encoding in ensembles of neurons, by revealing improved performance in the presence of CB1 receptor antagonists which increased the range of ensemble encoding on a trial-by-trial basis (Deadwyler et al., 2007). The results presented here support the above observations by demonstrating that CB1 receptor activation and inhibition alter intracellular calcium release provoked by excitatory synapses in hippocampus.

2. Methods

2.1. Hippocampal Slices

Preparation of hippocampal slices was similar to that described in previous reports (Hampson et al., 2003; Zhuang et al., 2005a; Zhuang et al., 2005b). Slices were obtained from Sprague-Dawley rats aged 10–17 days, following NIH guidelines. The brain was rapidly removed to a chilled (4°) oxygenated (95% O_2, 5% CO_2) artificial cerebrospinal fluid (ACSF) solution containing (mM) NaCl (126), $NaHCO_3$ (20), KCl (5), $MgCl_2$ (2), $CaCl_2$ (2.5), glucose (10), HEPES (20). Transverse slices (250–300 μm) were cut with a vibratome (Leica VT1000S); the hippocampus was dissected free and suspended in oxygenated ACSF at 30° for 1 hour.

Slices were transferred to a darkened Petri dish containing 13 μM Calcium Green acetoxymethyl ester-ACSF solution (50 μg Calcium Green 1 AM, Molecular Probes; reconstituted with 20% pluronic acid in dimethylsulfoxide (DMSO); Pluronic F-127, Molecular Probes) and incubated at room temperature with oxygenation for 45 min., rinsed in fresh ACSF and maintained in the dark at room temperature in oxygenated ACSF. Individual slices were then transferred to a temperature controlled recording chamber

(Warner Instruments; Hamden, CT), held in place with a harp slice anchor, and perfused continuously with gravity fed oxygenated ACSF solution at a rate of 1.8 ml/min.

2.2. Calcium Imaging

Imaging was performed on CA1 pyramidal cells with a Nikon E800 upright confocal microscope equipped with a water-immersion objective, a Hamamatsu-Orca-ER digital camera and a Perkin Elmer Ultraview spinning disc confocal system. The "Nipkow" spinning disk confocal technique provides rapid confocal imaging over a very large area, allowing subsecond imaging of a 1 millimeter square of tissue (Rutter et al., 2006). Calcium Green emission images (500–600 nm) were acquired using monochrome laser excitation at 488 nm with no emission wavelength filtering (Maravall et al., 2000). The images were stored at 0.3 s intervals, with a piezoelectric motor "stepping" the focal plane to acquire 40 vertical slices (2.5 μm depth) per field, thus producing a complete 3-D image every 12 sec. Images were "flattened," combining multiple depth slices, to allow analysis of whole neural soma captured in the 3-D confocal image. Intracellular calcium was assessed via change in cell soma fluorescence (ΔE, emission image density) plotted as a function of baseline (E_0) Calcium Green fluorescence (Paredes et al., 2008). The change in fluorescence, $\Delta E/E_0$, correlates to percentage change in intracellular calcium concentration (Maravall et al., 2000; Paredes et al., 2008; Wilms and Eilers, 2007) using single line laser excitation without requiring ratiometric measurement (e.g. Fura-2 (Paredes et al., 2008)). All slices were recorded and initially tested under baseline ACSF treatment conditions during which no change in intracellular calcium occurred (Step A – ACSF perfusion for 6.0 min.). They were then perfused with n-methyl-d-aspartic acid (NMDA) to elicit baseline intracellular calcium increases (Step B – ACSF perfusion for 3.0 min, 10 μM NMDA perfusion for 2 min, followed by ACSF for 5.0 min). To test the modulation of NMDA-elicited calcium, slices were pre-exposed to the experimental compound for 10.0 min via perfusion with media containing only the compound (Step C) then switched to media containing the compound + NMDA (concentration as in Step B) and exposed for 2.0 min, after which perfusion with media containing only the experimental compound was continued for an additional 5.0 min (Step D). Changes between the control ACSF solution and the experimental solutions were achieved by a solenoid valve switching system (Warner Instruments) to insure no interruption would occur in the perfusion of the slice. Confocal calcium imaging was continuous during Steps A–D to show the time course and percentage of change in NMDA-induced fluorescence following pre-exposure or reversal of effects of other (experimental) compounds.

2.3. Data Analysis

Changes in intracellular calcium dependent Calcium Green fluorescent image density (Figure 1A) were measured for Regions of Interest (ROIs) corresponding to CA1 cell soma (Figure 1B). The fluorescence change (ΔE) was divided by baseline fluorescence (E_0 – mean of first 120 seconds; Figure 1C) to normalize across cells and correct for photobleaching. Mean (percentage) $\Delta E/E_0$ across cells is plotted over time to indicate timecourse; the mean of peak % $\Delta E/E_0$ was statistically compared across cells using ANOVA. To ensure adequate sampling, a minimum of 3 cells (soma) were measured per hippocampal slice, with 5–10 slices tested for each treatment. All slices were tested with a minimum of one control (NMDA only) and one test drug, while some slices were tested with a second drug to assess blockade or reversal of the initial drug. In the latter case, control experiments showed no more than 5% variance in mean $\Delta E/E_0$ with repeated NMDA exposure, and complete washout of drug effects after 10 min perfusion.

2.4. Drug Preparation

The CB1 cannabinoid receptor antagonist rimonabant (SR141716A) was obtained from the National Institute on Drug Abuse (NIDA); all other drugs were obtained from commercial sources (Sigma-Aldrich and Tocris). Soluble drugs, NMDA, NBQX – 2,3-dihydroxy-6-nitro-7-sulfamoyl-benzo[f]quinoxaline-2,3-dione, CNQX – 6-cyano-7-nitroquinoxaline-2,3-dione, MK801 – (dizocilpine) (+)-5-methyl-10,11- dihydro-5*H*-dibenzo[*a*,*d*]cyclohepten-5,10-imine maleate), ryanodine, Sp-cAMPS – (Sp)-adenosine-3′, 5′-cyclic-*S*-(4-bromo-2,3-dioxobutyl)monophosphorothioate, Rp-cAMPS – (Rp)-adenosine-3′,5′-cyclic-*S*-(4-bromo-2,3-dioxobutyl)monophosphorothioate, PKA catalytic subunit, were prepared as dilutions in the ACSF bathing solution. Other drugs, WIN 55,212-2 – (R)-(+)-[2,3-Dihydro-5-methyl-3-(4-morpholinylmethyl)pyrrolo[1,2,3-de)-1,4-benzoxazin-6-yl]-1-napthalenylmethanone, Rimonabant – 5-(4-Chlorophenyl)-1-(2,4-dichloro-phenyl)-4-methyl-*N*-(piperidin-1-yl)-1*H*-pyrazole-3-carboxamide, AM281 – 1-(2,4-Dichlorophenyl)-5-(4-iodophenyl)-4-methyl-N-4-morpholinyl-1H-pyrazole-3-carboxamide, AM404 – N-(4-Hydroxyphenyl)-5Z,8Z,11Z,14Z-eicosatetraenamide, URB597 – (3′-(aminocarbonyl)[1,1′-biphenyl]-3-yl)- cyclohexylcarbamate, URB602 – [1,1′-biphenyl]-3-yl-carbamic acid, cyclohexyl ester, and JZL184 – 4-nitrophenyl-4-(dibenzo[d][1,3]dioxol-5- yl(hydroxy)methyl)piperidine-1-carboxylate were prepared as 10 mM stock in ethanol, then diluted in ACSF to final concentration and exposed to a constant stream of nitrogen to evaporate residual ethanol. All drugs were delivered by bath perfusion at 37°C.

3. Results

3.1. Cannabinoid receptors modulate neuronal calcium release

Slices of hippocampal tissue were saturated with Calcium Green AM (Sigma), and excited with a blue (488 nm) laser to fluorescence at intensity correlated with intracellular calcium concentrations. Figure 1A displays the measurement of calcium-dependent fluorescence as a function of NMDA exposure. The photomicrographs illustrate the peak fluorescence in response to NMDA and are color-coded to depict relative differences in intensity of cellular fluorescence for each of the conditions indicated. The photomicrograph in Figure 1B shows a portion of the field in Figure 1A to illustrate detection of cytosolic calcium in soma and dendrites by the Calcium Green fluorescence label. Calcium Green fluorescence is further quantified as the ratio of change in intensity relative to the baseline fluorescence ($\Delta E/E_0$) recorded for the 3.0 min prior to NMDA infusion (Figure 1C). Fluorescence is then plotted as mean (S.E.Ms. indicated by minimum and maximum error bars in Figure 1C) across regions of interest centered on each individual CA1 cell soma (red ellipse in Figure 1B, inset) for 3–8 neurons per slice, then repeated for 6–9 slices per treatment condition. Figure 1C shows that the standard dose of Rimonabant (5 μM) in the absence of NMDA in the perfusion medium exhibits no significant change in mean $\Delta E/E_0$ over the entire 10 min time period of exposure, however, Rimonabant in the bathing medium (2–10 μM) enhances NMDA-elicited intracellular calcium (NMDA: 30.9 ± 4.7%, NMDA+Rmbt 2 μM: 36.2 ± 4.4%, NMDA+Rmbt 5 μM: 50.7 ± 5.1%, NMDA+Rmbt 10 μM: 57.3 ± 3.9%, $F_{(2,672)} = 5.61$ $p<0.001$).

Figure 2A depicts the mean (±SEM) change in Calcium Green fluorescence produced by a brief (2 min) exposure to NMDA (10 μM) which was then modulated in the presence of cannabinoid receptor CB1 agonists (WIN) and antagonist (Rmbt) at different concentrations (n=19 slices, 56 cells measured). Ten minute pretreatment (Zhuang et al., 2005b) with the potent CB1 agonist WIN 55,212-2 (WIN, 5–25 μM) produced a significant concentration-related suppression the NMDA-elicited increase in intracellular calcium fluorescence as evidenced by the change in mean $\Delta E/E_0$ to 15.9 ± 5.8% compared to Control (i.e. NMDA alone) levels of 30.9 ± 4.7% ($F_{(1,672)} = 8.4–26.3$ $p<0.01- 0.001$; WIN 5–25 μM vs. Control).

The effects of WIN were blocked by co-administration of the CB1 antagonist rimonabant (Rmbt, 5 μM) which produced no significant change relative to the Control increase in fluorescence produced by NMDA alone (29.4 ± 5.8%, $F_{(1,672)} = 0.14$, n.s.). However, the basis for this suppression by the CB1 receptor antagonist was revealed by the fact that treatment with rimonabant alone significantly ($F_{(1,672)} = 28.4$, $p<0.001$) increased $\Delta E/E_0$ (50.7 ± 5.1), indicating the presence of endocannabinoids in the slice which acted to suppress NMDA induced changes in fluorescence from possible higher levels under Control conditions. The basis for this CB1 receptor mediated suppression of $\Delta E/E_0$ required further examination of NMDA receptor mediated release of intracellular Ca^{++} and where these two processes could interact.

To determine whether Rimonabant and WIN could be acting via multisynaptic pathways, the same experiments were conducted in the presence of tetrodotoxin (TTX, 100 nM). Figure 2B shows that Rimonabant administered alone continued to enhance the NMDA-elicited increase in intracellular calcium ($F_{(1,672)} = 22.9$, $p<0.001$) even when action potentials were blocked by TTX. Likewise Figure 2B shows that WIN-mediated decreases in NMDA induced calcium release, and blockade of WIN effects by Rimonabant were not significantly different ($F_{(2,672)} = 1.77$, n.s.) from results obtained in the absence of TTX (Figure 2A).

3.2. Calcium-dependent intracellular calcium release triggered by NMDA receptor activation

The NMDA elicited increase intracellular calcium was specific to activation of the NMDA receptor as shown by ruling out other glutamatergic receptor subtypes. Figure 2C shows that NBQX (20 μM), the AMPA receptor antagonist (Mateos et al., 2007), had no significant ($F_{(1,672)} = 2.0$, n.s.) effect on $\Delta E/E_0$ elicited by NMDA. In contrast, MK801 (20 μM), the NMDA receptor antagonist (Watson and Stanton, 2009), completely abolished the NMDA-elicited increase in intracellular calcium ($F_{(1,672)} = 54.8$, $p<0.001$). However, CNQX (20 μM), the AMPA/Kainate antagonist (Brickley et al., 2001) also significantly reduced NMDA-elicited $\Delta E/E_0$ from 32.2 ± 2.3% to 11.7 ± 1.6% ($F_{(1,672)} = 34.4$, $p<0.001$), most likely via the glycine binding site on the NMDA receptor (Lester et al., 1993; Li et al., 2009). Effects of Rmbt alone (Rmbt 5 μM) and NMDA + Rmbt on peak calcium fluorescence as in Figures 2A&B are shown for comparison. MK801 continued to block NMDA-elicited increases in intracellular calcium irrespective of whether Rmbt was co-administered ($F_{(1,672)} = 42.4$, $p<0.001$).

3.3. Influence of Extracellular Glycine on NMDA-elicited intracellular calcium flux

In Figure 2C the NMDA-elicited increase in intracellular calcium was attenuated by CNQX, implying possible influence of AMPA or glycine receptors (Brickley et al., 2001; Lester et al., 1993; Li et al., 2009). NBQX (20 μM) did not alter any of the above NMDA effects, ruling out AMPA/Kainate contributions. To test the contribution of extracellular glycine to the Rmbt-enhanced NMDA-elicited increase in intracellular calcium concentration, the effects of CNQX (20 μM) and glycine (5 μM) were assessed independently. In slices pretreated with CNQX, the NMDA produced 32.2 ± 2.3% increase in intracellular calcium (Figure 2C), was reduced to 11.7 ± 1.6% ($F_{(1,672)} = 34.4$, $p<0.001$). Also the Rmbt induced increase in NMDA-elicited calcium concentration to 50.7 ± 5.1% (Figure 2C) was reduced by the same concentration of CNQX to 44.5 ± 3.7% ($F_{(1,672)} = 7.83$, $p<0.01$). In contrast, NMDA+ glycine (5 μM) increased the calcium signal to 39.1 ± 3.4% ($F_{(1,672)} = 8.22$, $p<0.01$) vs. NMDA alone. Similarly glycine added to Rmbt + NMDA increased calcium concentration by a similar amount to 57.7 ± 4.6% ($F_{(1,672)} = 8.40$, $p<0.01$), compared to just NMDA+Rmbt. To assess the specificity of the influence of Rmbt relative to glycine in altering NMDA changes in calcium concentrations, NMDA was increased (18 μM) to produce the same change in intracellular calcium as NMDA + Rmbt (50.1 ± 4.7%). The

addition of glycine (5 μM) increased calcium levels to 58.0 ± 5.2% ($F_{(1,672)}$ = 9.36, p<0.01 vs. NMDA 18 μM alone) and CNQX (20 μM) decreased levels to 45.4 ± 4.8% ($F_{(1,672)}$ = 5.79, p<0.05 vs. NMDA 18 μM alone). The fact that the differential effect of glycine and CNQX on increased calcium produced by NMDA alone was similar to when the level of increase in NMDA was provoked by NMDA+Rmbt, allowed the dissection of the modifications in calcium levels into distinct NMDA-, glycine-, and Rmbt-sensitive components as shown in the inset in Figure 2C (compared to NMDA, 10 μM bar in Figure 2C). Finally, the effect of WIN (10 μM) shown in Figure 2A, when applied in the presence of 20 μM CNQX, completely suppressed the effect of NMDA on intracellular calcium (3.7 ± 1.6%, $F_{(1,672)}$ = 3.7, n.s. vs. ACSF), indicating a lack of CB1 controlled release of glycine.

3.4. Role of intracellular messengers regulating calcium-elicited calcium release

Verification that the NMDA-elicited $\Delta E/E_0$ resulted from intracellular release of calcium via ryanodine-sensitive (RyR) channels (Li et al., 2006; Unni et al., 2004; Zhuang et al., 2005b) is shown in Figure 3A where ryanodine (Ryano, 100 μM) significantly inhibited NMDA-elicited intracellular calcium release (Ryano: 8.4 ± 4.8% vs. Control 32.1 ± 4.3%, $F_{(1,672)}$ = 43.6, p<0.001). An important comparison showed that Rimonabant, which increased NMDA induced $\Delta E/E_0$ in Figure 1C, did not significantly increase $\Delta E/E_0$ in the presence of Ryanodine (14.9 ± 3.5%, $F_{(1,672)}$ = 3.7, n.s.).

Prior studies from this laboratory established that CB1 receptor modulation of potassium current is mediated by inhibition of cAMP-dependent protein kinase (protein kinase A, PKA) (Mu et al., 2000; Zhuang et al., 2005a). Calcium-elicited calcium release via RyR calcium channels requires phosphorylation of RyR by PKA (Yoshida et al., 1992); therefore we tested the effects of reciprocal modulation of PKA via Sp-cAMPS and Rp-cAMPS (Schafe and LeDoux, 2000; Xie and Lewis, 1997; Yamamoto et al., 2005). Figure 3B shows that Sp-cAMPS (20 μM) significantly increased $\Delta E/E_0$ (47.3 ± 3.6%, $F_{(1,672)}$ = 27.2, p<0.001), while Rp-cAMPS (20 μM) decreased $\Delta E/E_0$ (15.1 ± 4.0%, $F_{(1,672)}$ = 13.6, p<0.001). When co-administered with Rimonabant, Sp-cAMPS and Rp-cAMPS retained the same direction and magnitude of effect (Sp-cAMPS+Rmbt: 52.7 ± 5.4%, $F_{(1,672)}$ = 30.5, p<0.001; Rp-cAMPS+Rmbt: 17.4 ± 5.2%, $F_{(1,672)}$ = 10.9, p<0.001) indicating that the action of these specific PKA modulators was “downstream” from where activation of CB1 receptors by WIN decreased $\Delta E/E_0$ (Figure 2A) via inhibition of PKA.

3.5. Endogenous cannabinoids modulate NMDA-elicited intracellular calcium flux

The marked increase in NMDA induced $\Delta E/E_0$ elicited in the presence of Rimonabant could have been due to a) the putative “inverse agonist” effects of this compound at the CB1 receptor (Pertwee, 2005), or b) blockade of tonically released endogenous cannabinoids (Janero and Makriyannis, 2009; Martin-Garcia et al., 2010). The CB1 receptor antagonist AM281, with similar putative inverse agonist effects to rimonabant, likewise produced increased $\Delta E/E_0$ (Figure 4A) compared to Control (AM281: 50.9 ± 5.5%, Control: 32.0 ± 4.3%, $F_{(1,672)}$ = 25.7, p<0.001). Agents which prolong endocannabinoid action by inhibiting enzymatic degradation of endocannabinoids: AM404, URB597, URB602 and JZL184 (Abush and Akirav, 2009; Hajos et al., 2004; Karanian et al., 2005; Manwell et al., 2009; Pan et al., 2009), were tested to see if $\Delta E/E_0$ was decreased in a manner similar to WIN (Figure 2A). The fatty-acid amide hydrolase inhibitor URB597 (20 μM) decreased $\Delta E/E_0$ (14.7 ± 5.6%, $F_{(1,672)}$ = 21.4, p<0.001 vs. Control), as did the reuptake inhibitor AM404 (19.6 ± 3.7%, $F_{(1,672)}$ = 13.6, p<0.001 vs. Control). The MAG lipase inhibitors URB602 and JZL184 also decreased $\Delta E/E_0$ (URB602: 15.1 ± 6.3%, $F_{(1,672)}$ = 20.8, p<0.001; JZL184: 13.2 ± 4.1%, $F_{(1,672)}$ = 25.8, p<0.001 vs. Control). Rimonabant (5 μM) did not significantly increase $\Delta E/E_0$ in the presence of either AM404, URB597 or URB602 (Rmbt+AM404, URB597, URB602: ≤30 %, $F_{(1,672)}$ = 0.91, n.s. vs. AM404, URB597, URB602 alone).

However, increasing the concentration of rimonabant (10 μM) countered the additive effects of URB597 or URB602 plus endogenous cannabinoids, (Rmbt 10 μM+URB597 or Rmbt 10 μM+URB602: ≥47%, $F_{(1,672)} = 28.21$, $p<0.001$ vs. Control) and significantly enhanced $\Delta E/E_0$ in a manner similar to its effect (Figure 4B) in the absence of metabolic inhibitors (URB597, URB602). As in Figure 3, the inset confirms that the initial NMDA effects on $\Delta E/E_0$ were reproduced after washout of a prior NMDA+ drug combination, confirming a true reversal of AM404 and URB597/URB602 effects with no persistent change in response to perfusion with only NMDA. The facilitation at high concentration, and lack of facilitation at low concentrations of rimonabant in the presence of drugs that prolong the actions of endocannabinoids provides evidence for competitive effects at the CB1 receptor, and against inverse agonist effects of rimonabant on intracellular calcium mobilization.

4. Discussion

The demonstration here of the direct effect of CB1 receptor activation on NMDA triggered calcium release implicates endocannabinoids in the control of hippocampal cellular plasticity via modulation of the consequences of NMDA receptor-mediated calcium conductance. The fact that suppression of endogenous cannabinoid receptor activation alone enhances these effects (Figure 2A & 4A), is consistent with several recent reports showing interactions between synaptic efficacy and behavioral outcome as a function of levels of endocannabinoids and CB1 receptor activation, (Abush and Akirav, 2009; Li et al., 2009; Mateos et al., 2007; Watson and Stanton, 2009). However, the current findings indicate that NMDA receptor mediated release of intracellular calcium via RyR sensitive channels is modulated directly by inactivation of “tonically” active CB1 receptors.

NMDA or glutamate binding to NMDA receptors allows conductance of calcium with sodium ions (Shen and Johnson, 2010; Yang et al., 2010). The calcium influx in turn has been shown to bind to intracellular receptors such as ryanodine (RyR) receptors and result in enhanced release of calcium from intracellular stores (Christie and Jahr, 2008; Nosyreva and Kavalali, 2010; Unni et al., 2004). In this regard there are several mechanisms by which NMDA could enhance its own effect on pyramidal cells. For instance, presynaptic NMDA receptors (McGuinness et al., 2010) could release of additional glutamate which would bind to AMPA or NMDA channels, which would then be additive with postsynaptic NMDA receptors to enhance intracellular calcium in the postsynaptic cell. Blockade of presynaptic CB1 receptors on glutamatergic terminals via exposure to rimonabant (Rmbt) applied to glutamatergic terminals (Bhaskaran and Smith, 2010; Haj-Dahmane and Shen, 2010; Hoffman et al., 2010) could likewise enhance the effects of postsynaptic NDMA calcium influx by providing additional glutamatergic activation of pyramidal cells. However, the insensitivity of both the NMDA and Rmbt influences to TTX in the current studies, as well as the absence of elevated intracellular calcium resulting from application of Rmbt alone (Figure 5), argues against CB1 receptor regulation via electrically mediated synaptic actions.

Alternatively, CB1 or NMDA receptors on glial cells (Lee et al., 2010; Navarrete and Araque, 2010) could modulate release of glutamate or glycine (Hayashi et al., 2006; Winder et al., 1996; Yaguchi and Nishizaki, 2010) which could in turn activate or potentiate NMDA receptors on pyramidal cells. Blocking the glycine binding site on NMDA receptors via CNQX produced only a 10% reduction from the degree of change in calcium produced with Rmbt, irrespective of the presence of Rmbt. Also, the enhancement of NMDA effects by glycine under the same conditions was independent of the actions of Rmbt (Figure 2C, Inset) which as stated had no effect on calcium levels without NMDA present. Again, this does not rule out a contribution of extracellular NMDA and glycine release to a modulation of intracellular calcium by regulation of calcium influx through the NMDA receptor, however it does suggest that CB1-modulation of NMDA-elicited intracellular calcium is downstream

and independent of NMDA receptor gating on hippocampal pyramidal cells (Cakil et al., 2010; Liu et al., 2009).

An unexpected finding from this study is that modulation of synaptic actions of NMDA receptors by cannabinoids need not depend upon electrical activation of synapses containing CB1 receptors (Foldy et al., 2006; Hoffman and Lupica, 2000; Hofmann et al., 2008; Kim and Alger, 2010; Varma et al., 2002) but can also occur via endocannabinoid modulation of the intracellular consequences of calcium entry through NMDA receptors after they are activated. Figure 2C validates the fact that NMDA receptor activation *and* CB1 receptor blockade were necessary to induce an increase in intracellular calcium via RyR receptors. Since Rmbt alone had no effect Figure 5 illustrates a proposed intracellular pathway whereby concomitant activation of CB1 receptors, either by endocannabinoids or exogenous agonists (WIN), reduces production of adenylyl cyclase (AC) via inhibitory g-proteins (Gi), consequently reducing intracellular cAMP and levels of PKA (Howlett et al., 2010). A major functional impact of this reduction in PKA level is the corresponding decrease in phosphorylation of the calcium binding site on the RyR receptor (Figure 5). cAMP-dependent PKA phosphorylation of this calcium binding site on the RyR receptor enhances release of calcium, while de-phosphorylation via inhibition of cAMP reduces calcium binding, thereby reducing intracellular calcium release, and potentially reducing presynaptic neurotransmitter release (Katz, 1969) in axon terminals. Such decreased phosphorylation (AC-PKA-RyR in Figure 5) limits calcium binding and facilitated RyR release of intracellular calcium which can occur during NMDA receptor gated calcium influx (Figures 1–4).

The mechanism described in Figure 5 indicates that CB1 receptors were tonically active via endogenous cannabinoids in hippocampal slices in the resting state. Blockade of CB1 receptors in the absence of exogenously applied cannabinoids reduced the coincident inhibitory drive on AC produced by transient changes in levels of endocannabinoids, thereby increasing cAMP and PKA activation (Figure 3). Thereby the increased phosphorylation and facilitated binding of calcium to RyR via blockade of CB1 receptors resulted in the demonstrated increase in NMDA-elicited release of intracellular calcium by Rmbt shown in Figures 2–4.

The possibility of CB1-controlled synaptic pathways consistently modulating intracellular processes in pyramidal cells has been suggested by several recent findings. Derkinderen et. al (2003) demonstrated that CB1 receptor-mediated ERK activation was observed in hippocampal pyramidal cells. It has recently been shown that neocortical pyramidal neurons express CB1 receptors and modulate their own inhibition by synthesizing and releasing 2-AG which binds to CB1 receptors on the same neurons (Marinelli et al., 2009). Other evidence for a pyramidal cell locus for CB1 receptors was that knockout of CB1 receptors specifically on GABA neurons did not eliminate locomotor, hypothermic, analgesic and cataleptic responses to Δ-9-THC; however, deletion of the CB1 receptor on pyramidal cells eliminated these responses to cannabinoids (Monory et al., 2007). Finally, Isokawa (2009) showed that anandamide induced pCREB in pyramidal cells in slices. It is unlikely that this resulted from a multisynaptic action due to activation of presynaptic CB1 receptors on GABA neurons, because it has been established that anandamide is not responsible for DSI in hippocampal pyramidal neurons (Kim and Alger, 2004). The above studies demonstrate that CB1 receptors may be located at multiple loci on hippocampal neurons including presynaptic terminals, yet are self contained within hippocampal cells and do not necessarily require activation of multiple synapses functioning across a network of neurons (Robbe et al., 2006; Robbe and Buzsaki, 2009).

4.1. Conclusions

The significance of endocannabinoid modulatory processes has recently been shown for GABA mediated synaptic inhibition in chronic hippocampal slice cultures (Kim and Alger, 2010) and attest to the critical role of endocannabinoids with respect to regulating operation of hippocampal circuitry (Abush and Akirav, 2009; Kawamura et al., 2006; Mateos et al., 2007). Here we demonstrate the basis for a different modulatory action of endocannabinoids through a CB1 receptor coupled process that regulates the downstream effects of NMDA mediated excitatory glutamatergic synapses on release of intracellular calcium which provides a basis for recent findings showing endocannabinoid modulation of functional hippocampal processes (Deadwyler et al., 2007; Li et al., 2009; Watson and Stanton, 2009). Other investigations have shown that chronic activation or inhibition of cannabinoid receptors leads to persistent alterations in plasticity in hippocampus as well as other brain regions (Fowler et al., 2010; Karanian et al., 2005; Manwell et al., 2009; Martin-Garcia et al., 2010) which implies a functional role for endocannabinoids in state-dependent transient or repeated modulation of brain processes.

Investigations from this laboratory (Deadwyler et al., 2007; Deadwyler and Hampson, 2008) have shown how enhancement and suppression of trial-specific firing patterns in ensembles of hippocampal neurons associated with respective successful and deficient short-term memory in rodents, could have resulted from endocannabinoid modulation of NMDA mediated release of intracellular calcium shown here (Figure 5). This linkage was established by the fact that information encoded by ensembles on a trial-by-trial basis was negatively biased if endocannabinoid levels were increased causing a decrease in performance, while such biases could be reversed by CB1 receptor antagonists (Rmbt, AM281) which improved performance by increasing the encoding of task-related information (Deadwyler et al., 2007). The current findings demonstrate that endocannabinoid modulation of processes that increase intracellular calcium can occur downstream from the site of 1) glutamatergic synaptic depolarization and 2) the locus of agonist binding to cannabinoid (CB1) receptors. Such modulation can put performance at risk via reduced synaptic or cellular activity resulting in lack of synchronization of state-dependent firing required for modification of task behaviors based on trial-to-trial outcomes.

Acknowledgments

The authors thank Dr. Richard Rogers (Pennington Research Institute) for advice and technical assistance, and Dr. Allyn Howlett for helpful comments. This project was supported by NIH grants DA07625 to S.A.D. and DA08649 to R.E.H.

Abbreviations

ACSF	artificial cerebrospinal fluid
AM281	1-(2,4-Dichlorophenyl)-5-(4-iodophenyl)-4-methyl-N-4-morpholinyl-1H-pyrazole-3-carboxamide
AM404	N-(4-Hydroxyphenyl)-5Z,8Z,11Z,14Z-eicosatetraenamide
AMPA	(α-amino-3-hydroxyl-5-methyl-4-isoxazole-propionate
cAMP	3′,5′-cyclic adenosine monophosphate
CNQX	6-cyano-7-nitroquinoxaline-2,3-dione
DMSO	dimethylsulfoxide

JZL184	4-nitrophenyl-4-(dibenzo[d][1,3]dioxol-5- yl(hydroxy)methyl)piperidine-1-carboxylate
MK801	Dizocilpine: (+)-5-methyl-10,11- dihydro-5*H*-dibenzo[*a*,*d*]cyclohepten-5,10-imine maleate)
NBQX	2,3-dihydroxy-6-nitro-7-sulfamoyl-benzo[f]quinoxaline-2,3-dione
NMDA	n-methyl-d-aspartic acid
PKA	cAMP-dependent protein kinase
Rmbt	Rimonabant (original designation SR141716A): 5-(4-Chlorophenyl)-1-(2,4-dichlorophenyl)-4-methyl-*N*-(piperidin-1-yl)-1*H*-pyrazole-3-carboxamide
Rp-cAMPS	(Rp)-adenosine-3′,5′-cyclic-*S*-(4-bromo-2,3-dioxobutyl)monophosphorothioate
RyR	Ryanodine-sensitive intracellular calcium channel
Sp-cAMPS	(Sp)-adenosine-3′,5′-cyclic-*S*-(4-bromo-2,3-dioxobutyl)monophosphorothioate
TTX	tetrodotoxin – Octahydro-12-(hydroxymethyl)-2-imino-5,9:7,10a-dimethano-10aH-[1,3]dioxocino[6,5-d]pyrimidine-4,7,10,11,12-pentol
URB597	(3′-(aminocarbonyl)[1,1′-biphenyl]-3-yl)- cyclohexylcarbamate
URB602	[1,1′-biphenyl]-3-yl-carbamic acid, cyclohexyl ester
WIN	WIN 55,212-2:(R)-(+)-[2,3-Dihydro-5-methyl-3-(4-morpholinylmethyl)pyrrolo[1,2,3-de)-1,4-benzoxazin-6-yl]-1-napthalenylmethanone

References

Abush H, Akirav I. Cannabinoids modulate hippocampal memory and plasticity. Hippocampus. 2009

Bhaskaran MD, Smith BN. Cannabinoid-mediated inhibition of recurrent excitatory circuitry in the dentate gyrus in a mouse model of temporal lobe epilepsy. PLoS One. 2010; 5:e10683. [PubMed: 20498848]

Brickley SG, Farrant M, Swanson GT, Cull-Candy SG. CNQX increases GABA-mediated synaptic transmission in the cerebellum by an AMPA/kainate receptor-independent mechanism. Neuropharmacology. 2001; 41:730–736. [PubMed: 11640927]

Cakil D, Yildirim M, Ayyildiz M, Agar E. The effect of co-administration of the NMDA blocker with agonist and antagonist of CB1-receptor on penicillin-induced epileptiform activity in rats. Epilepsy Res. 2010

Chevaleyre V, Castillo PE. Heterosynaptic LTD of hippocampal GABAergic synapses: a novel role of endocannabinoids in regulating excitability. Neuron. 2003; 38:461–472. [PubMed: 12741992]

Christie JM, Jahr CE. Dendritic NMDA receptors activate axonal calcium channels. Neuron. 2008; 60:298–307. [PubMed: 18957221]

Deadwyler SA, Goonawardena AV, Hampson RE. Short-term memory is modulated by the spontaneous release of endocannabinoids: evidence from hippocampal population codes. Behav Pharmacol. 2007; 18:571–580. [PubMed: 17762525]

Deadwyler SA, Hampson RE. Endocannabinoids modulate encoding of sequential memory in the rat hippocampus. Psychopharmacology (Berl). 2008; 198:577–586. [PubMed: 18210094]

Derkinderen P, Valjent E, Toutant M, Corvol JC, Enslen H, Ledent C, Trzaskos J, Caboche J, Girault JA. Regulation of extracellular signal-regulated kinase by cannabinoids in hippocampus. J Neurosci. 2003; 23:2371–2382. [PubMed: 12657697]

Falenski KW, Blair RE, Sim-Selley LJ, Martin BR, DeLorenzo RJ. Status epilepticus causes a long-lasting redistribution of hippocampal cannabinoid type 1 receptor expression and function in the rat pilocarpine model of acquired epilepsy. Neuroscience. 2007; 146:1232–1244. [PubMed: 17433556]

Foldy C, Neu A, Jones MV, Soltesz I. Presynaptic, activity-dependent modulation of cannabinoid type 1 receptor-mediated inhibition of GABA release. J Neurosci. 2006; 26:1465–1469. [PubMed: 16452670]

Fortin DA, Trettel J, Levine ES. Brief trains of action potentials enhance pyramidal neuron excitability via endocannabinoid-mediated suppression of inhibition. J Neurophysiol. 2004; 92:2105–2112. [PubMed: 15175370]

Fowler CJ, Rojo ML, Rodriguez-Gaztelumendi A. Modulation of the endocannabinoid system: neuroprotection or neurotoxicity? Exp Neurol. 2010; 224:37–47. [PubMed: 20353772]

Glickfeld LL, Scanziani M. Distinct timing in the activity of cannabinoid-sensitive and cannabinoid-insensitive basket cells. Nat Neurosci. 2006; 9:807–815. [PubMed: 16648849]

Haj-Dahmane S, Shen RY. Regulation of plasticity of glutamate synapses by endocannabinoids and the cyclic-AMP/protein kinase A pathway in midbrain dopamine neurons. J Physiol. 2010; 588:2589–2604. [PubMed: 20498231]

Hajos N, Kathuria S, Dinh T, Piomelli D, Freund TF. Endocannabinoid transport tightly controls 2-arachidonoyl glycerol actions in the hippocampus: effects of low temperature and the transport inhibitor AM404. Eur J Neurosci. 2004; 19:2991–2996. [PubMed: 15182306]

Hampson RE, Zhuang SY, Weiner JL, Deadwyler SA. Functional significance of cannabinoid-mediated, depolarization-induced suppression of inhibition (DSI) in the hippocampus. J Neurophysiol. 2003; 90:55–64. [PubMed: 12649318]

Hashimotodani Y, Ohno-Shosaku T, Maejima T, Fukami K, Kano M. Pharmacological evidence for the involvement of diacylglycerol lipase in depolarization-induced endocanabinoid release. Neuropharmacology. 2008; 54:58–67. [PubMed: 17655882]

Hayashi Y, Ishibashi H, Hashimoto K, Nakanishi H. Potentiation of the NMDA receptor-mediated responses through the activation of the glycine site by microglia secreting soluble factors. Glia. 2006; 53:660–668. [PubMed: 16498631]

Hoffman AF, Laaris N, Kawamura M, Masino SA, Lupica CR. Control of cannabinoid CB1 receptor function on glutamate axon terminals by endogenous adenosine acting at A1 receptors. J Neurosci. 2010; 30:545–555. [PubMed: 20071517]

Hoffman AF, Lupica CR. Mechanisms of cannabinoid inhibition of GABA-A synaptic transmission in the hippocampus. J Neurosci. 2000; 20:2470–2479. [PubMed: 10729327]

Hofmann ME, Nahir B, Frazier CJ. Excitatory afferents to CA3 pyramidal cells display differential sensitivity to CB1 dependent inhibition of synaptic transmission. Neuropharmacology. 2008; 55:1140–1146. [PubMed: 18675282]

Howlett AC, Blume LC, Dalton GD. CB(1) cannabinoid receptors and their associated proteins. Curr Med Chem. 2010; 17:1382–1393. [PubMed: 20166926]

Isokawa M. Time-dependent induction of CREB phosphorylation in the hippocampus by the endogenous cannabinoid. Neurosci Lett. 2009; 457:53–57. [PubMed: 19429161]

Janero DR, Makriyannis A. Cannabinoid receptor antagonists: pharmacological opportunities, clinical experience, and translational prognosis. Expert Opin Emerg Drugs. 2009; 14:43–65. [PubMed: 19249987]

Karanian DA, Brown QB, Makriyannis A, Kosten TA, Bahr BA. Dual modulation of endocannabinoid transport and fatty acid amide hydrolase protects against excitotoxicity. J Neurosci. 2005; 25:7813–7820. [PubMed: 16120783]

Katz, B. The Release of Neural Transmitter Substances. Liverpool, UK: Liverpool University Press; 1969.

Kawamura Y, Fukaya M, Maejima T, Yoshida T, Miura E, Watanabe M, Ohno-Shosaku T, Kano M. The CB1 cannabinoid receptor is the major cannabinoid receptor at excitatory presynaptic sites in the hippocampus and cerebellum. J Neurosci. 2006; 26:2991–3001. [PubMed: 16540577]

Kim J, Alger BE. Inhibition of cyclooxygenase-2 potentiates retrograde endocannabinoid effects in hippocampus. Nat Neurosci. 2004; 7:697–698. [PubMed: 15184902]

Kim J, Alger BE. Reduction in endocannabinoid tone is a homeostatic mechanism for specific inhibitory synapses. Nat Neurosci. 2010; 13:592–600. [PubMed: 20348918]

Lee MC, Ting KK, Adams S, Brew BJ, Chung R, Guillemin GJ. Characterisation of the expression of NMDA receptors in human astrocytes. PLoS One. 2010; 5:e14123. [PubMed: 21152063]

Lester RA, Tong G, Jahr CE. Interactions between the glycine and glutamate binding sites of the NMDA receptor. J Neurosci. 1993; 13:1088–1096. [PubMed: 8095067]

Li XM, Gu Y, She JQ, Zhu DM, Niu ZD, Wang M, Chen JT, Sun LG, Ruan DY. Lead inhibited N-methyl-D-aspartate receptor-independent long-term potentiation involved ryanodine-sensitive calcium stores in rat hippocampal area CA1. Neuroscience. 2006; 139:463–473. [PubMed: 16457957]

Li Y, Krupa B, Kang JS, Bolshakov VY, Liu G. Glycine site of NMDA receptor serves as a spatiotemporal detector of synaptic activity patterns. J Neurophysiol. 2009; 102:578–589. [PubMed: 19439669]

Liu Q, Bhat M, Bowen WD, Cheng J. Signaling pathways from cannabinoid receptor-1 activation to inhibition of N-methyl-D-aspartic acid mediated calcium influx and neurotoxicity in dorsal root ganglion neurons. J Pharmacol Exp Ther. 2009; 331:1062–1070. [PubMed: 19752241]

Losonczy A, Biro AA, Nusser Z. Persistently active cannabinoid receptors mute a subpopulation of hippocampal interneurons. Proc Natl Acad Sci U S A. 2004; 101:1362–1367. [PubMed: 14734812]

Manwell LA, Satvat E, Lang ST, Allen CP, Leri F, Parker LA. FAAH inhibitor, URB-597, promotes extinction and CB(1) antagonist, SR141716, inhibits extinction of conditioned aversion produced by naloxone-precipitated morphine withdrawal, but not extinction of conditioned preference produced by morphine in rats. Pharmacol Biochem Behav. 2009; 94:154–162. [PubMed: 19698735]

Maravall M, Mainen ZF, Sabatini BL, Svoboda K. Estimating intracellular calcium concentrations and buffering without wavelength ratioing. Biophys J. 2000; 78:2655–2667. [PubMed: 10777761]

Marinelli S, Pacioni S, Cannich A, Marsicano G, Bacci A. Self-modulation of neocortical pyramidal neurons by endocannabinoids. Nat Neurosci. 2009; 12:1488–1490. [PubMed: 19915567]

Martin-Garcia E, Burokas A, Martin M, Berrendero F, Rubi B, Kiesselbach C, Heyne A, Gispert JD, Millan O, Maldonado R. Central and peripheral consequences of the chronic blockade of CB1 cannabinoid receptor with rimonabant or taranabant. J Neurochem. 2010; 112:1338–13351. [PubMed: 20028452]

Mateos JM, Luthi A, Savic N, Stierli B, Streit P, Gahwiler BH, McKinney RA. Synaptic modifications at the CA3-CA1 synapse after chronic AMPA receptor blockade in rat hippocampal slices. J Physiol. 2007; 581:129–138. [PubMed: 17303644]

McGuinness L, Taylor C, Taylor RD, Yau C, Langenhan T, Hart ML, Christian H, Tynan PW, Donnelly P, Emptage NJ. Presynaptic NMDARs in the hippocampus facilitate transmitter release at theta frequency. Neuron. 2010; 68:1109–1127. [PubMed: 21172613]

Monory K, Blaudzun H, Massa F, Kaiser N, Lemberger T, Schutz G, Wotjak CT, Lutz B, Marsicano G. Genetic dissection of behavioural and autonomic effects of Delta(9)-tetrahydrocannabinol in mice. PLoS Biol. 2007; 5:e269. [PubMed: 17927447]

Mu J, Zhuang SY, Hampson RE, Deadwyler SA. PKA-dependent phosphorylation and cannabinoid receptor modulation of potassium A-current (IA) in cultured rat hippocampal neurons. Pflugers Archiv - European Journal of Physiology. 2000; 439:541–546. [PubMed: 10764212]

Navarrete M, Araque A. Endocannabinoids potentiate synaptic transmission through stimulation of astrocytes. Neuron. 2010; 68:113–126. [PubMed: 20920795]

Nosyreva E, Kavalali ET. Activity-dependent augmentation of spontaneous neurotransmission during endoplasmic reticulum stress. J Neurosci. 2010; 30:7358–7368. [PubMed: 20505103]

Pan B, Wang W, Long JZ, Sun D, Hillard CJ, Cravatt BF, Liu QS. Blockade of 2-arachidonoylglycerol hydrolysis by selective monoacylglycerol lipase inhibitor 4-nitrophenyl 4-(dibenzo[d] [1,3]dioxol-5-yl(hydroxy)methyl)piperidine-1-carboxylate (JZL184) Enhances retrograde endocannabinoid signaling. J Pharmacol Exp Ther. 2009; 331:591–597. [PubMed: 19666749]

Paredes RM, Etzler JC, Watts LT, Zheng W, Lechleiter JD. Chemical calcium indicators. Methods. 2008; 46:143–151. [PubMed: 18929663]

Pertwee RG. Inverse agonism and neutral antagonism at cannabinoid CB1 receptors. Life Sci. 2005; 76:1307–1324. [PubMed: 15670612]

Robbe D, Buzsaki G. Alteration of theta timescale dynamics of hippocampal place cells by a cannabinoid is associated with memory impairment. J Neurosci. 2009; 29:12597–12605. [PubMed: 19812334]

Robbe D, Montgomery SM, Thome A, Rueda-Orozco PE, McNaughton BL, Buzsaki G. Cannabinoids reveal importance of spike timing coordination in hippocampal function. Nat Neurosci. 2006; 9:1526–1533. [PubMed: 17115043]

Rutter GA, Loder MK, Ravier MA. Rapid three-dimensional imaging of individual insulin release events by Nipkow disc confocal microscopy. Biochem Soc Trans. 2006; 34:675–678. [PubMed: 17052172]

Schafe, GE.; LeDoux, JE. J Neurosci. Vol. 20. 2000. Memory consolidation of auditory pavlovian fear conditioning requires protein synthesis and protein kinase A in the amygdala; p. RC96

Shen KZ, Johnson SW. Ca2+ influx through NMDA-gated channels activates ATP-sensitive K+ currents through a nitric oxide-cGMP pathway in subthalamic neurons. J Neurosci. 2010; 30:1882–1893. [PubMed: 20130197]

Unni VK, Zakharenko SS, Zablow L, DeCostanzo AJ, Siegelbaum SA. Calcium release from presynaptic ryanodine-sensitive stores is required for long-term depression at hippocampal CA3-CA3 pyramidal neuron synapses. J Neurosci. 2004; 24:9612–9622. [PubMed: 15509748]

Varma N, Brager D, Morishita W, Lenz RA, London B, Alger B. Presynaptic factors in the regulation of DSI expression in hippocampus. Neuropharmacology. 2002; 43:550–562. [PubMed: 12367601]

Watson DJ, Stanton ME. Intrahippocampal administration of an NMDA-receptor antagonist impairs spatial discrimination reversal learning in weanling rats. Neurobiol Learn Mem. 2009; 92:89–98. [PubMed: 19248837]

Wilms CD, Eilers J. Photo-physical properties of Ca2+-indicator dyes suitable for two-photon fluorescence-lifetime recordings. J Microsc. 2007; 225:209–213. [PubMed: 17371443]

Wilson RI, Kunos G, Nicoll RA. Presynaptic specificity of endocannabinoid signaling in the hippocampus. Neuron. 2001; 31:453–462. [PubMed: 11516401]

Winder DG, Ritch PS, Gereau RW, Conn PJ. Novel glial-neuronal signalling by coactivation of metabotropic glutamate and beta-adrenergic receptors in rat hippocampus. J Physiol. 1996; 494 (Pt 3):743–755. [PubMed: 8865071]

Xie CW, Lewis DV. Involvement of cAMP-dependent protein kinase in mu-opioid modulation of NMDA-mediated synaptic currents. J Neurophysiol. 1997; 78:759–766. [PubMed: 9307110]

Yaguchi T, Nishizaki T. Extracellular high K+ stimulates vesicular glutamate release from astrocytes by activating voltage-dependent calcium channels. J Cell Physiol. 2010; 225:512–518. [PubMed: 20506270]

Yamamoto M, Urakubo T, Tominaga-Yoshino K, Ogura A. Long-lasting synapse formation in cultured rat hippocampal neurons after repeated PKA activation. Brain Res. 2005; 1042:6–16. [PubMed: 15823247]

Yang YC, Lee CH, Kuo CC. Ionic flow enhances low-affinity binding: a revised mechanistic view into Mg2+ block of NMDA receptors. J Physiol. 2010; 588:633–650. [PubMed: 20026615]

Yoshida A, Ogura A, Imagawa T, Shigekawa M, Takahashi M. Cyclic AMP-dependent phosphorylation of the rat brain ryanodine receptor. J Neurosci. 1992; 12:1094–1100. [PubMed: 1312134]

Zhuang S, Hampson RE, Deadwyler SA. Behaviorally relevant endocannabinoid action in hippocampus: dependence on temporal summation of multiple inputs. Behav Pharmacol. 2005a; 16:463–471. [PubMed: 16148452]

Zhuang SY, Bridges D, Grigorenko E, McCloud S, Boon A, Hampson RE, Deadwyler SA. Cannabinoids produce neuroprotection by reducing intracellular calcium release from ryanodine-sensitive stores. Neuropharmacology. 2005b; 48:1086–1096. [PubMed: 15910885]

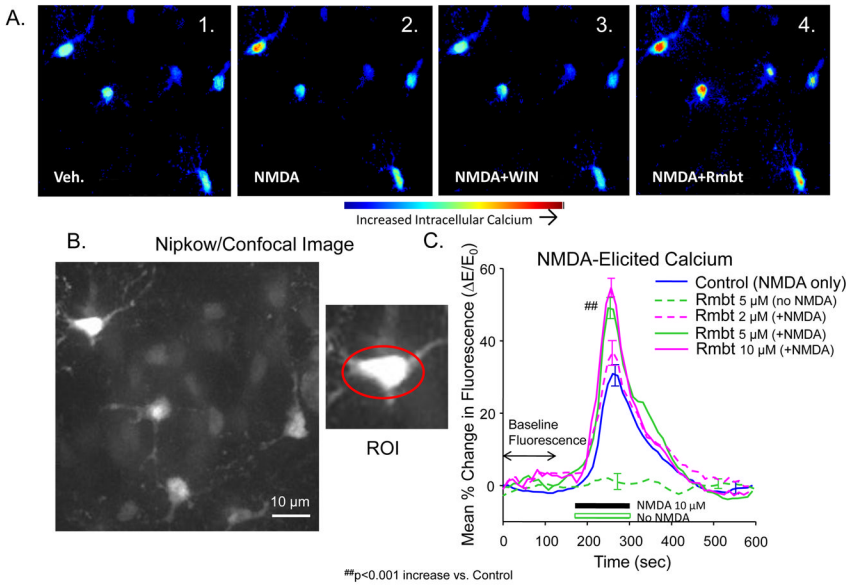

Figure 1.

NMDA-elicited increases in intracellular calcium analyzed from confocal imaged cells in hippocampal slices. Mean percent change in Calcium Green fluorescence is linearly correlated to mean percent change in intracellular calcium concentration (Maravall et al., 2000; Paredes et al., 2008). **A:** Color-coded photomicrographs of laser confocal imaging of Calcium Green fluorescence in the CA1 layer of *in vitro* rat hippocampal slices. Squares indicate the same field of 5 neurons from the same hippocampal slice under peak fluorescence for the conditions graphed in C: 1 – Vehicle (ACSF) exposure only; 2 – NMDA exposure, 3 – NMDA in presence of WIN; 4 – NMDA in presence of rimonabant. Color-coding of image indicates fluorescent intensity as shown in color calibration bar: blue: background fluorescence/intracellular calcium concentration, yellow: 20%, red: >40% $\Delta E/E_0$. Range: 20–40% change in intracellular calcium concentration (as $\Delta E/E_0$). **B:** Enlarged photomicrographs of upper left portion of field in A shows neural soma and dendrites revealed by Calcium Green fluorescence. Inset (right) shows setting of a typical Region of Interest (ROI), namely an ellipse positioned to include the complete soma and base of the dendrites. Intracellular calcium changes were determined by mean relative change in fluorescent image intensity density of regions of interest (ROIs) centered on cell bodies located in the CA1 cell layer shown in A. ROIs corresponding to CA1 soma were indentified for 3–8 neurons per slice, drug treatments were repeated for 6–9 slices each. **C:** Change in fluorescence, and hence intracellular calcium, produced by NMDA exposure plotted as a function of percentage of baseline fluorescence ($\Delta E/E_0$). Trace indicates mean (max and min S.E.M. indicated by error bars) $\Delta E/E_0$ over the following three phases of confocal image assessment: ***(i)*** 3 minute exposure to normal (in artificial cerebrospinal fluid, ACSF) medium, (***ii***) 2 min perfusion of NMDA (10 μm, black bar on horizontal axis), and (***iii***) 5 min washout with re-exposure to normal medium. Vertical deflections indicate calcium release from intracellular stores elicited by calcium influx through NMDA receptor channels as shown by the blue curve for Control exposures (NMDA only). The lower green curve shows $\Delta E/E_0$ for slices exposed to Rmbt without the simultaneous NMDA perfusion (No NMDA). Modulation of NMDA-elicited change in intracellular calcium is demonstrated by increased calcium produced by CB1 antagonist rimonabant (Rmbt, 2–10 μM). Hash marks (##p<0.001) indicate significant increases in peak $\Delta E/E_0$ from Control. Slice and cell quantities were: Control: 19 slices, 56 cells; Rmbt (5 μM) alone: 9 slices, 23 cells; NMDA

+Rmbt 2μM: 6 slices; 19 cells; NMDA+Rmbt: 5 μM: 9 slices, 36 cells; NMDA+Rmbt: 10 μM: 5 slices, 18 cells.

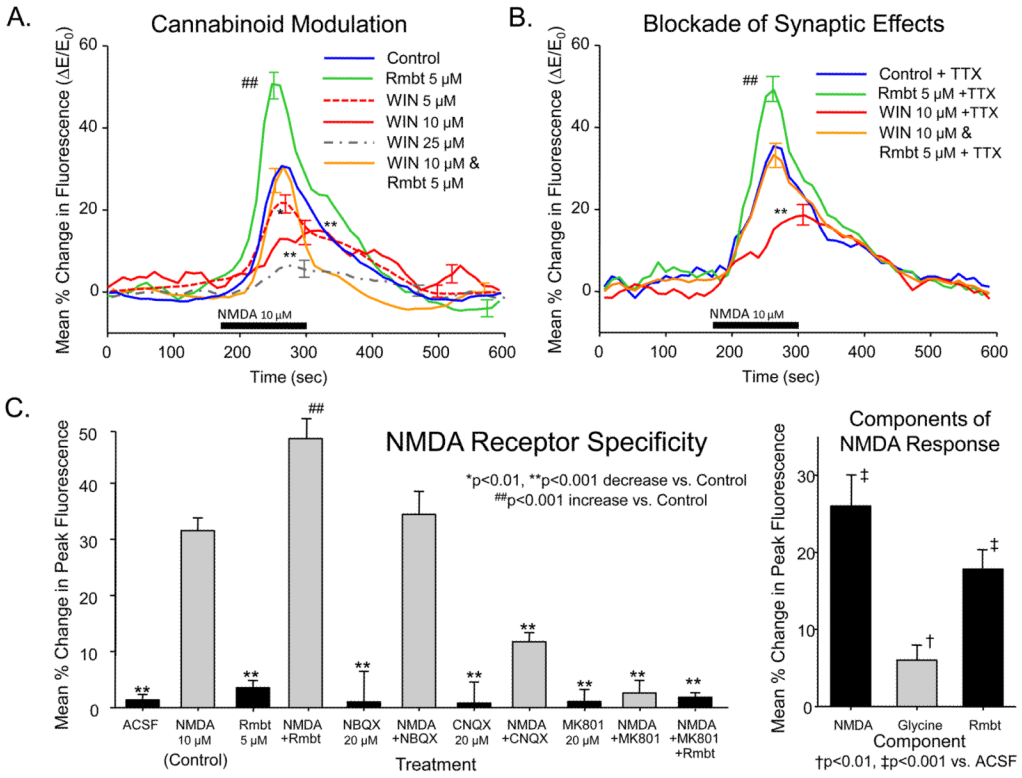

Figure 2.

Modulation of NMDA-elicited changes in intracellular calcium. **A**: Modulation by cannabinoid CB1 receptors. CB1 antagonist rimonabant (Rmbt, 5 μM), CB1 agonist WIN 55,212-2 (WIN 5, 10, 25 μM) and bathing medium containing WIN (10 μM) plus Rmbt (5 μM) are shown as different colored plots. Asterisks (**p<0.001) indicate significant decreases in peak $\Delta E/E_0$ from Control. Hash marks (##p<0.001) indicate significant increases in peak $\Delta E/E_0$ from Control. Slice and cell quantities were: Control: 19 slices, 56 cells; Rmbt: 9 slices, 36 cells; WIN 5 μM: 8 slices, 23 cells; WIN 10 μM: 10 slices, 35 cells WIN 25 μM: 7 slices, 20 cells; WIN 10 μM & Rmbt: 9 Slices, 36 cells. **B**: CB1 modulation of NMDA-elicited changes in intracellular calcium were not dependent on action potential generation. CB1 antagonist rimonabant (Rmbt, 5 μM), CB1 agonist WIN 55,212-2 (WIN 5, 10, 25 μM) and WIN (10 μM) plus Rmbt (5 μM) were tested with tetrodotoxin (100 nM) in the bathing medium to block action potentials and rule out multisynaptic network influences. Asterisks and hash marks indicate significant difference in peak $\Delta E/E_0$ from Control as in A. Slice and cell quantities were: Control+TTX: 11 slices, 41 cells; Rmbt+TTX: 6 slices, 28 cells; WIN+TTX: 5 slices, 17 cells; WIN&Rmbt+TTX: 6 Slices, 21 cells. **C**: NMDA receptor-dependent changes in Calcium Green fluorescence. Bar graph indicates mean (± S.E.M.) peak of $\Delta E/E_0$ measured during 2 min perfusion of glutamatergic antagonists alone and in combination with NMDA. Hippocampal slices were exposed to NMDA (10 μM, Figure 1C) with the 1) AMPA receptor antagonist NBQX (20 μM), 2) AMPA/Kainate receptor antagonist CNQX (20 μM), and 3) NMDA receptor antagonist MK801 (20 μm). Rmbt alone and in combination with NMDA and MK801 shown for comparison with Figure 1C. Asterisks (**p<0.001) indicate significant reductions in peak $\Delta E/E_0$ from Control/ NMDA only (green bar). Significant decrease in NMDA-elicited $\Delta E/E_0$ by above antagonists likely resulted from actions of high concentrations of CNQX at the glycine binding site on NMDA receptors (red bar). Slice and cell quantities: Control/ACSF and NMDA only: 22 slices, 67 cells; NBQX and NBQX+NMDA: 6 slices, 21 cells; CNQX and

CNQX+NMDA: 8 slices, 24 cells; MK801 and MK801+NMDA: 8 Slices, 22 cells; Rmbt alone: 9 slices, 23 cells; NMDA+Rmbt 9 slices, 36 cells; NMDA+Rmbt+MK801: 7 slices, 21 cells. Inset (right): Relative contribution of NMDA, glycine and Rmbt which correspond to the total change in fluorescence produced by NMDA+Rmbt in the barograph at left. Proportions were obtained by testing NMDA in combination with CNQX (20 μM) or glycine (5 μM) along with Rmbt (5 μM) or NMDA at higher concentration (18 μM) to mimic Rmbt effects (see Section 3.2). Independently varying increments of fluorescence increase correspond to NMDA receptor activation (NMDA), activation of glycine binding site on NMDA receptors (glycine), and blockade of endocannabinoid activation of CB1 receptor (Rmbt).

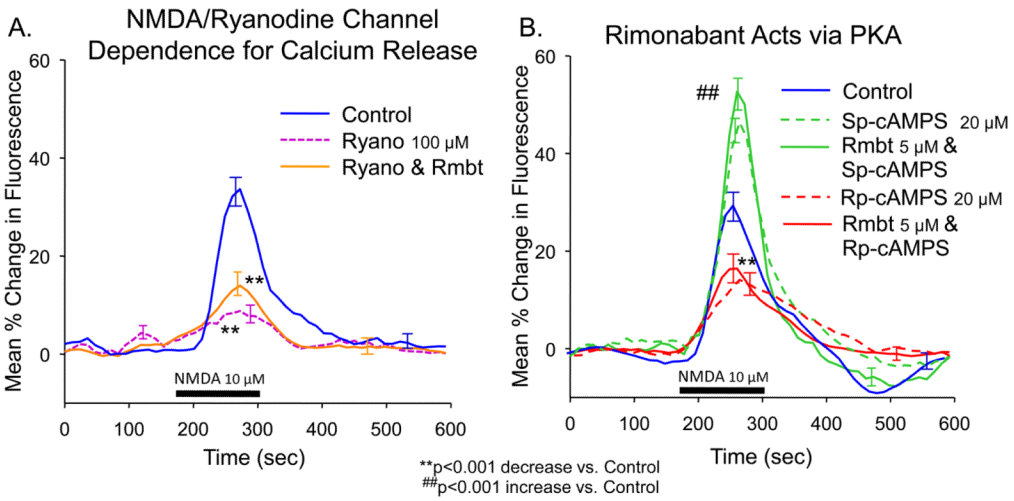

Figure 3.

Modulation of NMDA-elicited release of intracellular calcium. **A.** Ryanodine (Ryano) sensitive intracellular calcium release. Traces indicate mean $\Delta E/E_0$ (largest and smallest S.E.M. as in Figure 1A) produced following perfusion with Ryano (100 μM), which blocked release of calcium from endoplasmic reticulum via ryanodine-sensitive channels. Rimonabant (Rmbt, 5 μM) did not significantly increase $\Delta E/E_0$ in the presence of ryanodine. Asterisks (**p<0.001) indicate significance difference in peak $\Delta E/E_0$ from Control. All measurements were made on the same 9 slices, 33 cells. **B:** PKA regulatory subunit reciprocally modulates intracellular calcium release. Traces show biphasic modulation of $\Delta E/E_0$ produced by Sp and Rp stereoisomer's of nonhydrolyzable cAMP thioate (Sp-cAMPS, Rp-cAMPS, 20 μM) which respectively activate or inhibit PKA activity. Rimonabant in combination with Sp-cAMPS or Rp-cAMPS produced no significant additional change in intracellular calcium concentration. Asterisks (**p<0.001) indicate significantly decreased peak $\Delta E/E_0$ from Control. Hash marks (##p<0.001) indicate significant increases in peak $\Delta E/E_0$ from Control. Slice and cell quantities: Control: 13 slices, 47 cells; Sp-cAMPS and Sp-cAMPS+Rmbt: 6 slices, 28 cells; Rp-cAMPS and Rp-cAMPS+Rmbt: 7 slices, 19 cells.

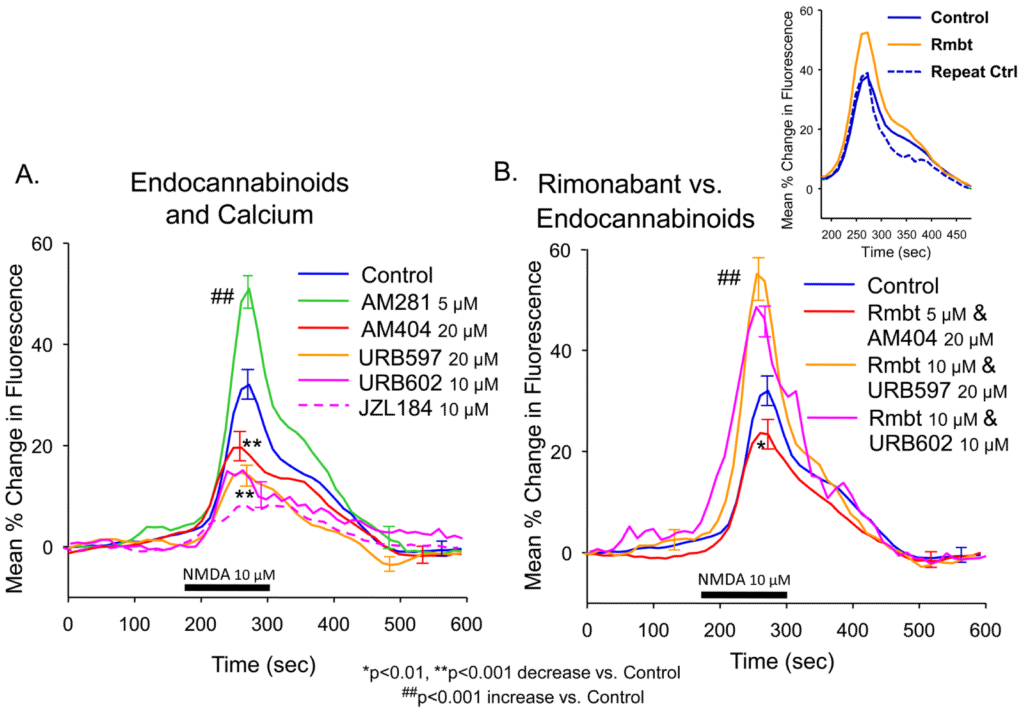

Figure 4.

Interaction of endogenous cannabinoids with intracellular calcium flux. **A.** Increasing endocannabinoid receptor action reduces $\Delta E/E_0$ similar to WIN (Figure 1C). Hippocampal slices were pretreated with the fatty-acid amide hydrolase inhibitors URB597 (20 μM) and AM404 (20 μM) as well as MAG lipase inhibitors URB602 (10 μM) and JZL184 (10 μM) to prolong agonist effects of endogenously-released cannabinoids at the CB1 receptor. Traces indicate mean reduction in NMDA elicited $\Delta E/E_0$ (max/min S.E.M) following pretreatment with the above agents. In contrast, pretreatment with a different CB1 receptor antagonist, AM281 (5 μM), produced enhancement of $\Delta E/E_0$, similar to rimonabant (Figures 1C). Significant decrease or increase in peak $\Delta E/E_0$ from Control (NMDA only) indicated by Asterisks (**p<0.001) and Hash marks (##p<0.001) respectively. Slice and cell quantities: Control: 24 slices, 80 cells; AM404: 8 slices, 29 cells; URB597: 7 slices, 25 cells; URB602: 8 slices, 29 cells; JZL184: 5 slices, 16 cells; AM281: 9 slices, 26 cells. **B:** Co-exposure of Rmbt with AM404, URB597 and URB602 suggests that rimonabant competes with endocannabinoids to increase levels of intracellular calcium. Traces show competition of AM404 and Rmbt co-perfused at the customary dose. A higher dose of Rmbt (10 μM), was required to reverse URB597 and URB602. Significant decrease or increase in peak $\Delta E/E_0$ from Control indicated by Asterisk (*p<0.01) or Hash marks (##p<0.001) respectively. Slice and cell quantities: Control: 24 slices, 80 cells; AM404+Rmbt: 8 slices, 29 cells; URB597+Rmbt 10 μM: 6 slices, 20 cells; URB602+Rmbt 10 μM: 8 slices, 25 cells. **Inset:** Repeated testing within the same slices. Graph compares 8 slices, 32 cells that were re-tested with exposure only to NMDA (Repeated Control) after washout of rimonabant that caused the initial change in peak $\Delta E/E_0$. Mean peak $\Delta E/E_0$ for the repeated NMDA exposure in the same slices as in B did not vary significantly (≤5%) from the initial (Control) exposure.

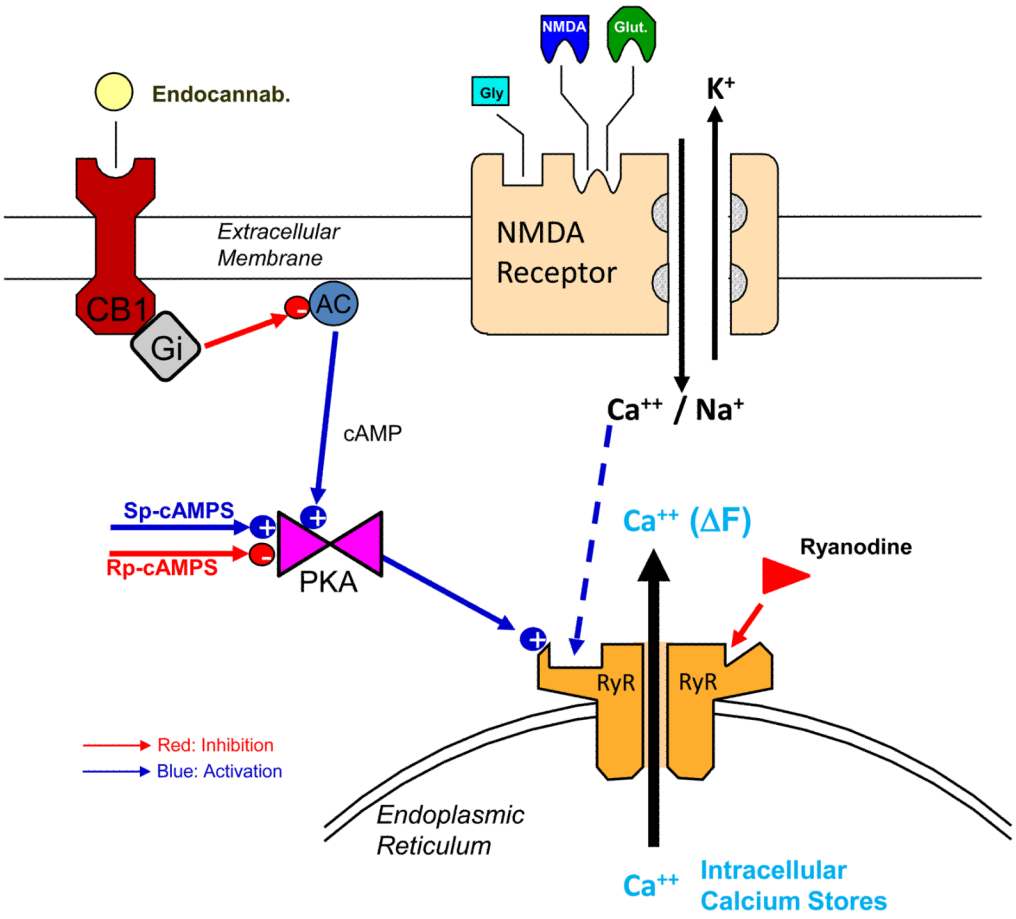

Figure 5.

Diagram showing proposed mechanism for endocannabinoid modulation of NMDA receptor mediated release of intracellular calcium. NMDA receptor illustrated with binding sites for glutamate, NMDA and glycine. Gating of receptor channel via glutamatergic transmission allows inward conductance of sodium (Na^+) and calcium (Ca^{++}) and outward movement of potassium (K^+) ions. Calcium entering the cell via glutamate/NMDA-activated channels binds to phosphorylated calcium binding sites on the ryanodine receptor-sensitive intracellular calcium channel (RyR). Such calcium binding facilitates RyR mediated release of calcium from endoplasmic reticulum to elevate free intracellular calcium levels as detected by $\Delta E/E_0$. RyR are negatively modulated by ryanodine (red arrow) and positively modulated by phosphorylation (blue arrow and plus sign) of the calcium RyR binding site which is mediated by the catalytic subunit of cAMP dependent protein kinase (PKA). PKA is in turn activated by increased 3′, 5′ cyclic adenosine monophosphate (cAMP) levels produced by adenylyl cyclase (AC). PKA is reciprocally modulated by thio esters of cAMP (Sp-cAMPS and Rp-cAMPS) shown by opposite (+ or −) signs on PKA in the diagram. Activation of cannabinoid receptors (CB1) by endocannabinoids produces inhibition of AC synthesis via the inhibitory g-protein subunit (Gi). Inhibition of AC results in decreased cAMP which leads to decreased PKA activity which reduces phosphorylation of RyR resulting in a reduction in release of intracellular calcium in response to synaptic activation NMDA receptors. Given this direct effect of CB1 receptor activation, a contrasting enhancement of NMDA-elicited intracellular calcium release resulting from blockade of tonic inhibition by resting levels of endocannabinoids in hippocampus, would be expected

following administration of a CB1 receptor antagonist, as demonstrated here in Rimonabant treated slices (Figures 1–4).